



MINISTRY OF SUPPLY

AERONAUTICAL RESEARCH COUNCIL
REPORTS AND MEMORANDA

Supersonic Wind-Tunnel Flutter Tests of Two Rectangular Wings

By

P. R. GUYETT, B.Sc.

© *Crown copyright 1958*

LONDON: HER MAJESTY'S STATIONERY OFFICE

1958

PRICE 5s. 6d. NET

Supersonic Wind-Tunnel Flutter Tests of Two Rectangular Wings

By

P. R. GUYETT, B.Sc.

COMMUNICATED BY THE DIRECTOR-GENERAL OF SCIENTIFIC RESEARCH (AIR),
MINISTRY OF SUPPLY

*Reports and Memoranda No. 3080**

May, 1956

Summary.—Two rectangular wings of aspect ratio 4 were flutter tested in a supersonic wind tunnel at Mach numbers 1.6 and 2.0 using a technique in which a structural stiffness was varied to give flutter at the Mach number. The results are in reasonable agreement with calculations using theoretical three-dimensional derivatives and arbitrary wing modes, though in general the calculated critical stiffnesses are rather higher than the test values. It is shown theoretically that structural damping has an important effect upon the stiffness required to avoid flutter, and may in some circumstances be destabilising.

1. *Introduction.*—Over the past few years, the prediction of flutter characteristics at supersonic speeds has become increasingly important in aircraft and missile design. Flutter calculations are normally based on equations which represent the overall balance of forces occurring in the interaction of two or more natural modes of vibration. In the evaluation of the sets of forces involved it is recognised that the aerodynamic forces present the greatest difficulty. The accuracy of theoretical estimates of these forces is limited by the assumptions, and generally aerofoil thickness, viscosity and shock waves are ignored. There is evidence¹ that these are significant, and experimental aerodynamic-force measurements are clearly required. Of more urgent importance, however, is experimental evidence on whether conventional calculations, using such theoretical aerodynamic derivatives as are available, give realistic flutter speeds. This information can most readily be obtained by flutter-testing models in wind tunnels, and a series of tests is described in this report.

The tests were made with two half-span rectangular wings of aspect ratio 4 in an intermittent type supersonic wind tunnel at Mach numbers of 1.6 and 2.0. Use of a tunnel in which wind speed and density had to remain constant during an experiment meant that subsonic procedure in which wind speed is adjusted to produce flutter could not be followed. Instead, the wings were mounted on a pitching axle in the tunnel wall and the wing pitching stiffness reduced until flutter occurred†. Comparative calculations were then made for each test configuration using arbitrary modes, based on the resonance characteristics of the wings, and theoretical derivatives. The calculated and experimental critical stiffnesses and frequencies are in reasonable agreement, with the calculated stiffnesses, in general, rather higher than the test values. This result is in agreement with the conclusions of Nelson and Rainey², who have made calculations to compare

* R.A.E. Report Struct. 206, received 18th October, 1956.

† The rig was designed by Mr. W. G. Molyneux of Structures Department, R.A.E.

with the supersonic wind-tunnel flutter tests of Tuovila, Baker and Regier³, at Langley Aeronautical Laboratory. The present report also shows that structural damping has an important effect on the calculated stiffnesses and frequencies for the test wings, and that structural damping in pitch can be destabilising.

2. *Apparatus.*—2.1. *Wind Tunnel.*—The tests were made in the 9 in. Supersonic Tunnel at the Royal Aircraft Establishment Ball Hill site. The tunnel is of the intermittent type, allowing a test run of approximately 40 seconds duration. The tunnel Mach number is determined by the shape of the liner forming the bottom face of the rectangular working-section. One of the vertical walls was used as a mounting for the model and the opposite wall held an observation window.

The air speeds and densities at the test Mach numbers are given in Table 1.

2.2. *Wing Models.*—The wings were of rectangular plan-form having a semi-span of 6 in. and a chord of 3 in. Each wing had a thickness/chord ratio of 0.05 and was of RAE 104 section profile. A rectangular-section root block extended over the full chord of the wings. Further details of the wings are given in Table 2.

Three wings were made, from solid Duralumin, magnesium alloy, and Permalin (a compressed wood).

2.3. *Wing Support and Pitching Spring.*—The wing mounting and the method of varying the pitching stiffness are shown diagrammatically in Fig. 1. Measured spring stiffnesses are plotted against roller position in Fig. 6. The roller carriage was driven by an actuator, which was remotely controlled and operated a Desyn indicator showing the position of the roller carriage on a dial on the remote control box. The position of the wing pitching axis was altered by moving the wing root block in the fork-end fitting of the pitching axle. The wing support, roller carriage, the actuator and Desyn indicator were mounted on the outside of the removable working-section wall. Fig. 2 shows the arrangement.

To prevent airflow through the aperture at the wing root from outside the wind tunnel into the low-pressure working section, the equipment on the removable wall was enclosed in a sealing cover. The wall, cover, remote-control box and one of the wings are shown in Fig. 3.

2.4. *Safety Catch.* An automatic safety catch was fitted to arrest the pitching bar when its amplitude exceeded a predetermined value. The catch is shown in position in Fig. 2. The method of operation may be followed from Fig. 4, which shows the catch in the locked position. Pulling the Bowden-cable wire causes the resetting lever to pivot about the ledge on the trigger and lift against the main tension spring. This disengages the pitching bar from its slot in the arresting lever. The catch is held in this position by a ratchet on a lever operating the cable wire (not shown in Fig. 4). The pitching bar is now free to oscillate until it touches the triggering bolt. At larger amplitudes the triggering bolt and trigger are displaced and the ledge support is withdrawn from the resetting lever. The tension spring then pulls down the arresting lever, which clamps the pitch bar in its slot. The fall of the arresting lever operates a micro-switch which stops the traverse of the actuator. The catch may be brought to the priming position again by releasing the ratchet holding the Bowden cable, whereupon the compression spring inside the sealing cover pulls the wire down and allows the resetting lever to engage on the ledge.

The triggering bolt was set to allow the pitching bar (and hence the wing) a free amplitude of ± 1 deg.

2.5. *Oscillation Recorder.*—A microphone pick-up close to the pitch bar gave an output signal proportional to the pitching displacement. This signal was displayed on a twin-beam oscilloscope together with the signal from a 1,000 c.p.s. oscillator. A continuous camera record was made of the traces during each test run, which enabled the form and frequency of the oscillation to be determined.

3. *Flutter Tests*.—The flutter condition for each wing configuration was found by steadily reducing the pitching stiffness with the tunnel operating until flutter developed. For the first test run in each configuration the flutter was allowed to trigger the safety catch and stop the roller carriage to indicate the region of critical stiffness. In subsequent tests this region was approached slowly and the wing tip observed through a telescope to detect the onset of flutter. The critical stiffness was taken to be the maximum stiffness at which a flutter oscillation, of small amplitude, developed. Reduction of stiffness below this value caused the amplitude to grow and trigger the safety catch. The flutter frequency was found from the oscilloscope camera record. The critical flutter pitching stiffness was found from the wing pitching frequency in still air. This frequency was obtained by disturbing the wing in pitch and recording the decaying oscillation. To avoid exciting the fundamental bending mode the wing tip was held on the pitching axis.

Tests using this technique were made on the Duralumin and magnesium-alloy wings with the pitching axis at the leading edge and at the quarter-chord at Mach numbers of 1.6 and 2.0. Flutter within the available test range of stiffness was found in five of the eight configurations. In one of the remaining three conditions (the Duralumin wing pitching about its leading edge at $M = 1.6$) the camera record showed an irregular oscillation which indicated that the wing may have been close to a flutter condition.

Although the safety catch prevented the development of excessive wing loads during a flutter oscillation, the models were subject to large and unavoidable transient loads from shock waves while the flow was being established and being shut off. The Permali wing was broken in stopping the tunnel before any flutter information was obtained from it. The magnesium-alloy wing was also broken in stopping the tunnel but fortunately after its test programme was complete. The Duralumin wing appeared to be unaffected by the loading.

4. *Flutter Calculations*.—Flutter calculations were made following the method described by Templeton⁴. The equations, however, were solved for pitching stiffness and frequency parameter, to conform to the test conditions.

The modes used in the calculations were rigid wing pitch about the pitching axis together with two arbitrary distortion modes. The distortion modes were chosen to relate the resonance nodal positions and frequencies of the test wings to the modal shapes of a uniform beam, as follows :

- (1) From the position of the nodal line in the lowest torsional resonance mode of the Duralumin wing (*see* Fig. 5) a spanwise reference axis was determined $0.43c$ behind the leading edge. This axis position was taken to be the nodal line for an arbitrary torsional mode (mode 1) having the modal shape of the first torsional mode of a uniform beam.
- (2) A primarily bending mode was then found by combining the fundamental bending mode and first torsional mode of a uniform beam to give a mode having no coupling inertia with the torsion mode at (1).

The modes (1) and (2) above were based on the resonance modes of the Duralumin wing in the calculations on both the Duralumin and magnesium-alloy wings, as the magnesium-alloy wing was destroyed in the flutter tests before its torsional resonance mode was found. For the same reason the frequency in the derived torsional mode (1) was made equal to the frequency of the lowest torsional mode of the Duralumin wing for both sets of calculations. Since the stiffness/weight ratios of Duralumin and magnesium alloy are almost the same the wing modes and frequencies should be practically identical and thus the assumption made should not involve significant error. The frequency in the derived bending mode (2), however, was made equal to the appropriate wing fundamental bending frequency in the wall mounting.

Inertias in the modes were found by integration using measured values of wing density. The inertia of the wing mounting and pitching spring in the rigid-body pitching mode was found for each of the flutter test conditions from measurements of the change of pitching frequency when known masses were added to the pitch bar.

The aerodynamic-force coefficients were calculated using theoretical derivatives due to Acum⁵. The derivatives apply to rectangular wings oscillating in rigid modes of pitch and normal translation. In the absence of other information these derivatives were treated as equivalent constant-strip derivatives in evaluating aerodynamic coefficients for the distortion modes.

Calculations were made for each test condition in the two degrees of freedom rigid-body pitch and the bending mode (2) above. The results are given in Table 3. Further calculations including all three degrees of freedom were made for two test configurations. The effect of adding structural damping was also investigated and some results are plotted in Figs. 7 and 8. The ternary flutter equations and the binary equations involving structural damping were solved on the R.A.E. Flutter Simulator.

5. *Discussion of Experimental and Calculated Results.*—5.1. *Direct Comparison.*—The experimental frequency parameters and stiffnesses are given together with the results of the two-degrees-of-freedom calculations excluding structural damping (*see* Section 4) in Table 3.

It may be seen that the Duralumin wing at $M = 1.6$ and $M = 2.0$ and the magnesium-alloy wing at $M = 2.0$ fluttered with the pitching-axis position at the quarter-chord but did not flutter with the axis at the leading edge, and that the magnesium-alloy wing at $M = 1.6$ fluttered at both axis positions. The calculations showed flutter in all the conditions in which it was found experimentally but also showed flutter in two of the three configurations in which it was not obtained experimentally. The two configurations are the Duralumin wing at $M = 1.6$ and the magnesium-alloy wing at $M = 2.0$, both with axis positions at the leading edge. Further calculations were made for these wings in the purely theoretical condition in which the pitching axis was a quarter-chord distance ahead of the leading edge. In this condition the calculations showed that the wings were free from flutter. A similar calculation made for the magnesium-alloy wing at $M = 1.6$, with which flutter was obtained experimentally at both axis positions showed flutter also with the axis a quarter-chord in front of the leading edge. Thus the calculations correctly predict the trend of the experimental results, and show that the wings are free from flutter at a forward axis position in those conditions in which the wings did not flutter experimentally with the axis at the leading edge. The calculations, however, are conservative in as much that they show flutter for two conditions which were free from flutter in the tests.

The results also enable a detailed comparison to be made of the experimental and calculated stiffnesses and frequencies in the five test conditions in which flutter occurred. This shows that the calculated frequencies are from 6 to 16 per cent higher than the measured frequencies and the calculated critical stiffnesses are from 4 per cent below to 51 per cent above the measured stiffnesses. The general tendency for the calculated stiffnesses to be above the measured stiffnesses implies a margin of safety in calculations for the test-wing conditions.

Calculations were also made for two test conditions taking account of structural damping in pitch and including the torsional degree of freedom at (1) in Section 4. The resulting critical stiffnesses and frequency parameters are shown in Figs. 7 and 8. Throughout the range of variation of damping the effect of including the torsional mode is negligibly small. Adding structural damping, however, produces important reductions in both critical-stiffness and flutter frequency parameter. For the test damping coefficients, the reductions in calculated frequency are 11 per cent and 7 per cent and the final frequencies are in close agreement with the experimental values. For the magnesium-alloy wing the change in calculated stiffness obtained by including structural damping reduces the amount by which the theoretical stiffness exceeds the measured value from 51 per cent to 20 per cent. For the Duralumin wing, which was the only wing condition having the theoretical critical stiffness below the measured stiffness, the change reduces the theoretical stiffness from 4 per cent below the measured value to 13 per cent below. Since the addition of damping appears to reduce both the theoretical critical stiffness and the frequency, its general effect, for all the wings that fluttered, should be to improve the agreement between the measured and calculated stiffnesses and frequencies.

A calculation including damping in both the pitching and bending modes was made for the Duralumin wing with pitching axis at the leading edge at $M = 1.6$, which in the tests showed an irregular apparently low damped oscillation but did not flutter (*see* Section 3). Damping in this condition also reduced the theoretical critical stiffness, but did not suppress flutter.

5.2. Effect of Varying Direct Pitching Inertia.—In addition to the above comparison of calculated and test flutter stiffnesses the particular form of the apparatus allows the stiffnesses to be compared at values of the direct pitching inertia other than those at which the tests were made. The direct pitching inertia includes the contribution of the pitch bar and axle, pitching spring and root-end fitting as well as the wing itself. These root components oscillate in the single degree of freedom of pitch and therefore do not provide a cross inertia with any mode or direct inertia in any other mode. It is thus physically possible to vary the direct inertia in the pitching mode without affecting any other inertia coefficients in the flutter equations. Since the direct inertia (A) and stiffness (E) in pitch occur together in the equations in a combined term ($-\omega^2 A + E$), ω being the flutter frequency, it is clear that if an increase δA in A is accompanied by an increase $\delta E = \omega^2 \delta A$ in E , then the equations give an otherwise identical flutter condition. For a given critical flutter condition, therefore, a change in the direct pitching inertia produces only a change in the critical pitching stiffness according to the linear variation $\delta E/\delta A = \omega^2$.

Variation of the critical pitching stiffness with pitching inertia for each wing condition in which flutter occurred is shown in Figs. 9 and 10. The theoretical line is for the two-degree-of-freedom system with zero damping. The experimental line refers to a condition in which the coefficient of structural damping in pitch is constant. Since the value of the critical damping coefficient decreases as the pitching inertia decreases*, it follows that the fraction of critical damping in pitch increases as the pitching inertia is decreased.

In Fig. 9 and 10 the rate of decrease of critical stiffness with pitching inertia ($\delta E/\delta A$) is greater for the calculated flutter condition than for the corresponding experimental condition, the calculated flutter frequency being higher than the measured frequency in each case. The effect of this for some conditions is to cause the theoretical predicted flutter pitching stiffness to fall below the measured stiffness at low values of pitching inertia. Thus the theoretical analysis with zero damping in pitch generally underestimates the stiffness required to prevent flutter at pitching inertias corresponding to the wing alone, whereas at the higher test inertia conditions the theoretical analysis generally overestimates the required stiffness. It should be noted, however, that if the calculated and measured frequencies coincide, then the margin between the calculated and experimental stiffnesses would be maintained independently of the pitching inertia. For the two wing conditions in which the effect of adding structural damping in pitch was examined (Figs. 7 and 8), it was found that the calculated and measured frequencies agreed closely and thus the discrepancy between the calculated and measured stiffnesses would be the same at all values of pitching inertia instead of varying with pitching inertia as shown in Figs. 9b and 9c.

The effects of adding structural damping in pitch at the bare wing inertia condition for the magnesium-alloy wing and the Duralumin wing, both with the pitching axis at the quarter chord at $M = 1.6$, can be deduced from Figs. 7 and 9b, and Figs. 8 and 9c, respectively. In each case addition of damping produces an increase in the critical pitching stiffness. This contrasts with the results at the test inertia conditions (Figs. 7 and 8), where addition of damping caused a decrease in the critical stiffness. A detailed examination of the effect of structural damping on the critical stiffness of the Duralumin wing showed that the increase in critical stiffness due to adding damping in pitch could be counteracted by adding structural damping in the flexural mode. Thus in practice, where structural damping is present in all modes, an increase in critical stiffness due to damping may not occur. Nevertheless, these results show the importance of structural damping and indicate that, in some circumstances, it can have a significant destabilising effect.

* The critical damping coefficient = $2\sqrt{(\text{pitching inertia} \times \text{pitching stiffness})}$.

5.3. *Flutter at Subsonic Speeds.*—To obtain an indication of the subsonic flutter characteristics of the wings, a single binary calculation was made for the Duralumin wing having the pitching axis at the quarter chord, at an air density corresponding to $M = 1.6$. The wing was given a pitching stiffness equal to the theoretical pitching stiffness at $M = 1.6$ as found in the calculations described in Section 4. Aerodynamic-force coefficients were evaluated from two-dimensional derivatives at $M = 0$. The equations were then solved for flutter speed and frequency parameter, and gave a flutter speed equivalent to a Mach number of unity. This answer is not, of course, exact since the derivatives are inappropriate, but it does indicate that the wings would be free from flutter at least until high subsonic speeds.

6. *Conclusions.*—Supersonic wind-tunnel flutter tests have been made using a technique in which the pitching stiffness of a half-span model wing mounted on a pitching axle in the tunnel wall was reduced until flutter occurred. Two rectangular wings of aspect ratio 4 were tested in this way, each at Mach numbers of 1.6 and 2.0 and each with pitching-axis positions at the wing leading edge and the quarter-chord. Flutter, involving modes mainly of pitch and wing bending, was found in five of the eight test configurations. The three configurations in which flutter was not found were all with the pitching axis at the leading edge.

Flutter calculations using arbitrary modes and theoretical derivatives were made for each test condition, and a comparison with the experimental results yielded the following facts :

- (a) The calculations correctly predicted flutter in all the five configurations in which it occurred but also showed flutter in two of the leading-edge pitching-axis configurations which were flutter free. However, additional calculations for these two cases showed freedom from flutter at a further forward position of the pitching axis. The calculations thus reproduce the experimental trend, indicating that the wings were generally less susceptible to flutter at forward pitching axis positions.
- (b) The calculated critical stiffnesses for the wings that fluttered were within the range 4 per cent below to 51 per cent above the corresponding measured stiffnesses and the calculated frequencies between 6 and 16 per cent above the measured frequencies. Calculations including the measured structural damping in pitch were made for the two extreme conditions of critical stiffness quoted above, and the calculated stiffnesses were altered from 4 per cent below to 13 per cent below and from 51 per cent above to 20 per cent above the measured stiffnesses. The revised frequencies agreed almost exactly. Since the calculated stiffnesses were, in all but one instance, above the measured stiffnesses, and the frequencies above the measured frequencies, the general effect of including structural damping in the calculations is to improve the agreement between theory and experiment.
- (c) The particular form of the apparatus allowed the experimental and calculated results to be compared at any value of the direct pitching inertia. At a reduced value of the pitching inertia corresponding to that of the bare wing it was shown that structural damping in pitch can have a destabilising effect.

7. *Further Development.*—A corresponding series of tests is to be made on a family of wings of delta plan-form.

8. *Acknowledgement.*—The author wishes to acknowledge the help given by members of the Aerodynamics Department, R.A.E., who operated the tunnel for these tests.

REFERENCES

<i>No.</i>	<i>Author</i>	<i>Title, etc.</i>
1	M. D. Van Dyke	Supersonic flow past oscillating airfoils including non-linear thickness effects. N.A.C.A. Tech. Note 2982. July, 1953.
2	H. C. Nelson and R. A. Rainey	Comparison of flutter calculations using various aerodynamic coefficients with experimental results for some rectangular cantilever wings at Mach number 1.3. N.A.C.A. Tech. Note 3301. November, 1954.
3	W. J. Tuovila, J. E. Baker and A. E. Regier.	Initial experiments on flutter of unswept cantilever wings at Mach number 1.3. N.A.C.A. Tech. Note 3312. November, 1954.
4	H. Templeton	The technique of flutter calculations. C.P. 172. April, 1953.
5	W. E. A. Acum	Aerodynamic forces on rectangular wings oscillating in a supersonic wind-stream. R. & M. 2763. August, 1950.

TABLE 1

Tunnel Wind Speeds and Air Densities

Speeds given in ft/sec ; density in slug/ft³

Mach number	Speed	Density
1.6	1456	8.46×10^{-4}
2.0	1659	5.47×10^{-4}

TABLE 2

Wing Details

Wing chord = 3 in. Wing semi-span = 6 in.

Distance of c.g. from leading edge = 1.33 in.

Radius of gyration of section about spanwise axis through c.g. = 0.688 in.

Wing mass/unit span :

Duralumin wing : $0.0311 \frac{\text{lb}}{\text{in}}$

Magnesium alloy wing : $0.0202 \frac{\text{lb}}{\text{in}}$

Wing fundamental bending frequency :

Duralumin wing 106 c.p.s.

Magnesium-alloy wing 105 c.p.s.

TABLE 3

Measured and Calculated Pitching Stiffnesses and Frequency Parameters

Pitching stiffness quoted in $\frac{\text{lb/ft}}{\text{radn}}$

Frequency parameter, $\nu = \omega c/V$,

where ω = flutter circular frequency

c = wing chord

V = wind speed.

Ratios given are $\frac{\nu \text{ (expt.)}}{\nu \text{ (calculated)}}$ and $\frac{\text{Pitching stiffness (expt.)}}{\text{Pitching stiffness (calculated)}}$.

(a) *Duralumin Wing at M = 1.6*

(i) Axis of pitch at quarter chord.

Total direct pitching inertia = 0.888 lb/in.².

	ν	Ratio	Pitching stiffness	Ratio
Experiment ..	0.128	$\frac{1}{1.06}$	124	$\frac{1}{0.96}$
Calculated ..	0.136		119	

(ii) Axis of pitch at leading edge.

Total direct pitching inertia = 1.381 lb/in.².

Experimental record showed irregular oscillations but no well defined flutter.

	ν	Pitching stiffness
Calculated ..	0.127	118

(iii) Axis of pitch quarter-chord distance ahead of leading edge.

Theoretical condition only.

Total direct pitching inertia assumed = 1.5 lb/in.².

Flutter not found at real positive values of pitching stiffness.

(b) *Magnesium-Alloy Wing at M = 1.6*

(i) Axis of pitch at quarter chord.

Total direct pitching inertia = 1.318 lb/in.².

	ν	Ratio	Pitching stiffness	Ratio
Experiment ..	0.130	$\frac{1}{1.13}$	138	$\frac{1}{1.51}$
Calculated ..	0.147		208	

(ii) Axis of pitch at the leading edge.

Total direct pitching inertia = 1.66 lb/in.².

	ν	Ratio	Pitching stiffness	Ratio
Experiment ..	0.125	$\frac{1}{1.16}$	167	$\frac{1}{1.32}$
Calculated ..	0.145		221	

TABLE 3—continued

(iii) Axis of pitch quarter-chord distance ahead of the leading edge.

Theoretical condition only.

Total direct pitching inertia assumed = 1.5 lb/in.².

	r	Pitching stiffness
Calculated ..	0.130	110

(c) Duralumin Wing at $M = 2.0$

(i) Axis of pitch at quarter-chord.

Total direct pitching inertia = 1.241 lb/in.².

	r	Ratio	Pitching stiffness	Ratio
Experiment ..	0.105	1	136	1
Calculated ..	0.115	1.10	148	1.09

(ii) Axis of pitch at the leading edge.

Total direct pitching inertia = 1.381 lb/in.².

No flutter found under test.

No flutter found theoretically at real positive pitching stiffness.

(d) Magnesium-Alloy Wing at $M = 2.0$

(i) Axis of pitch at quarter-chord.

Total direct pitching inertia = 0.792 lb/in.².

	r	Ratio	Pitching stiffness	Ratio
Experiment ..	0.107	1	93	1
Calculated: ..	0.121	1.13	105	1.13

(ii) Axis of pitch at leading edge.

Total direct pitching inertia = 1.124 lb/in.².

No flutter found experimentally.

	r	Pitching stiffness
Calculated ..	0.111	103

(iii) Axis of pitch quarter-chord distance ahead of leading edge.

Theoretical condition only.

Total direct pitching inertia assumed = 1.5 lb/in.².

Flutter not found at real positive values of pitching stiffness.

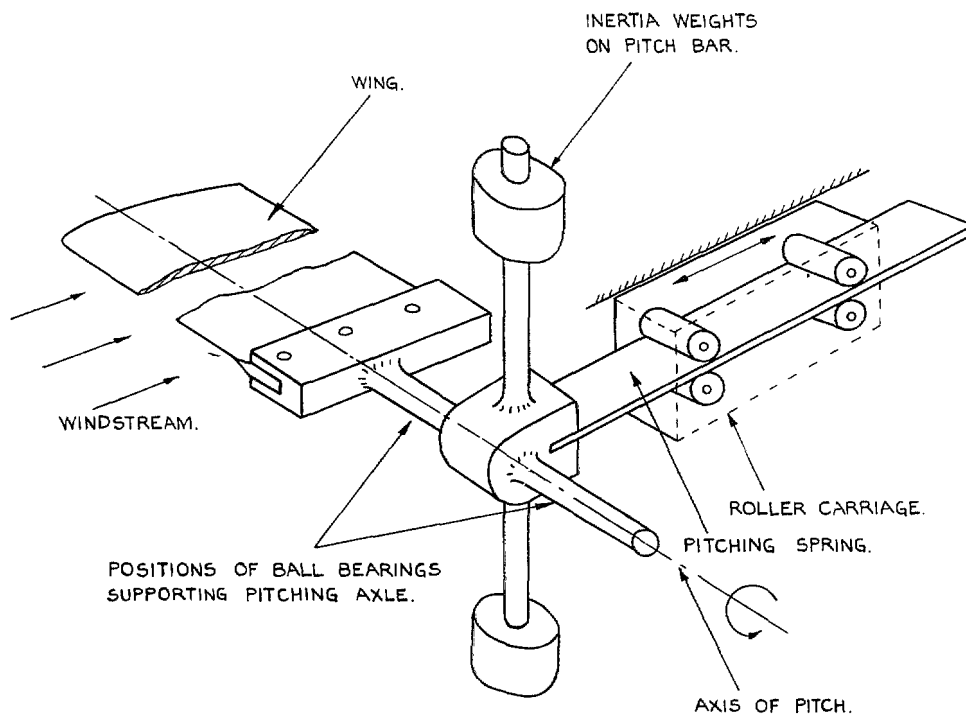


FIG. 1. Diagram of rig.

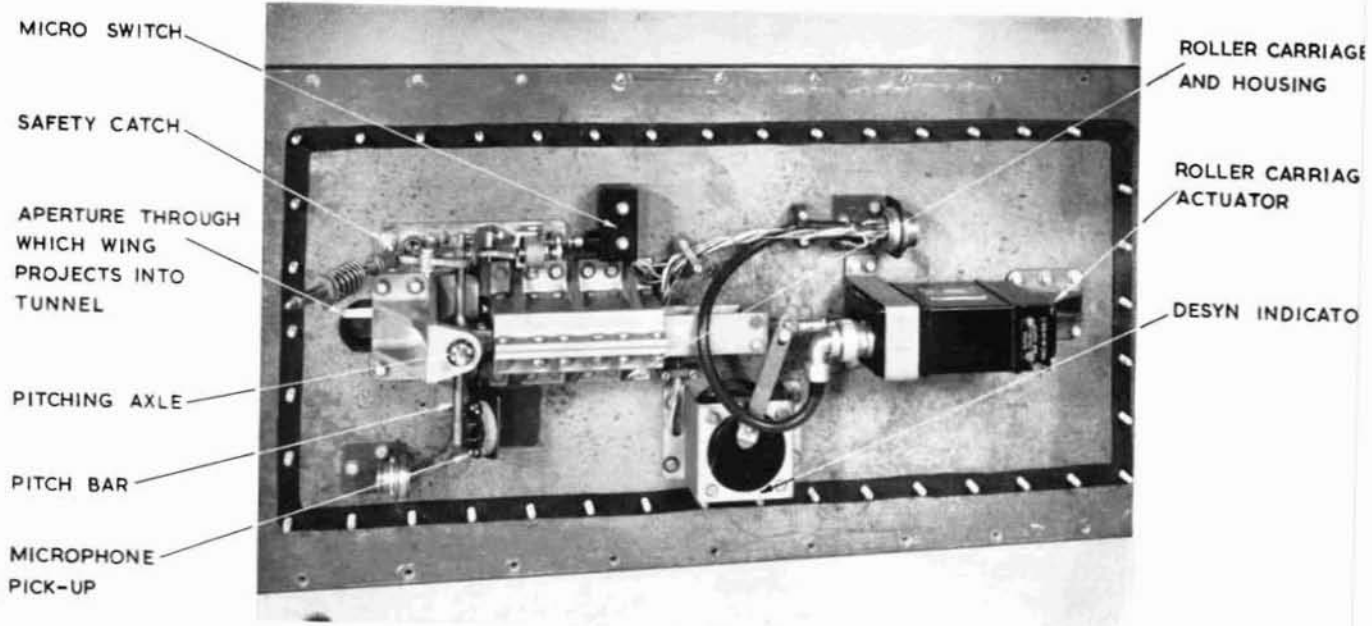


FIG. 2. Wing mounting.

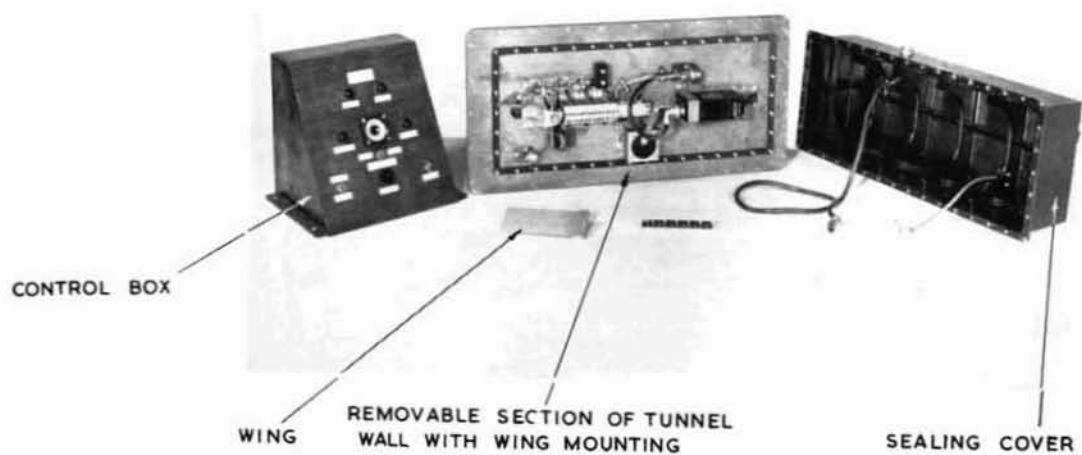


FIG. 3. Test equipment.

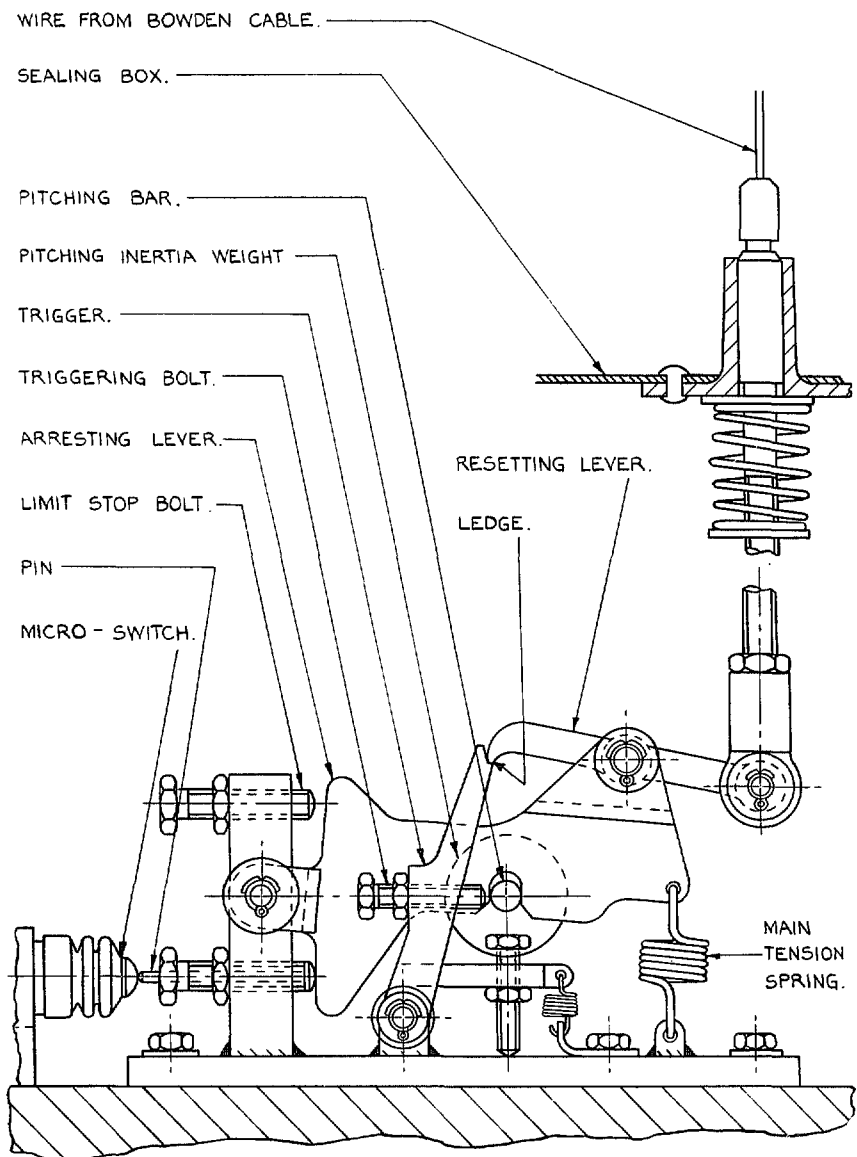


FIG. 4. Safety catch.

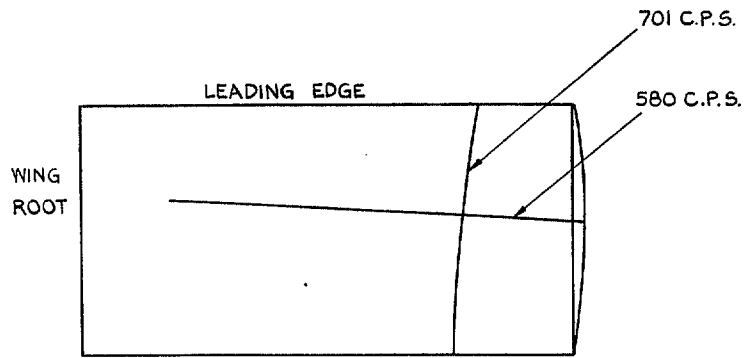


FIG. 5. Duralumin-wing nodal lines.

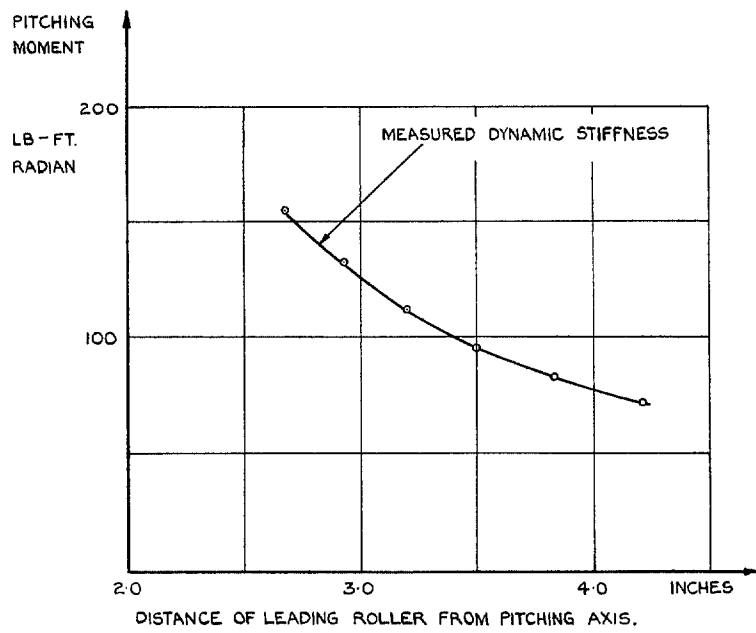


FIG. 6. Variation of pitching stiffness with roller position.

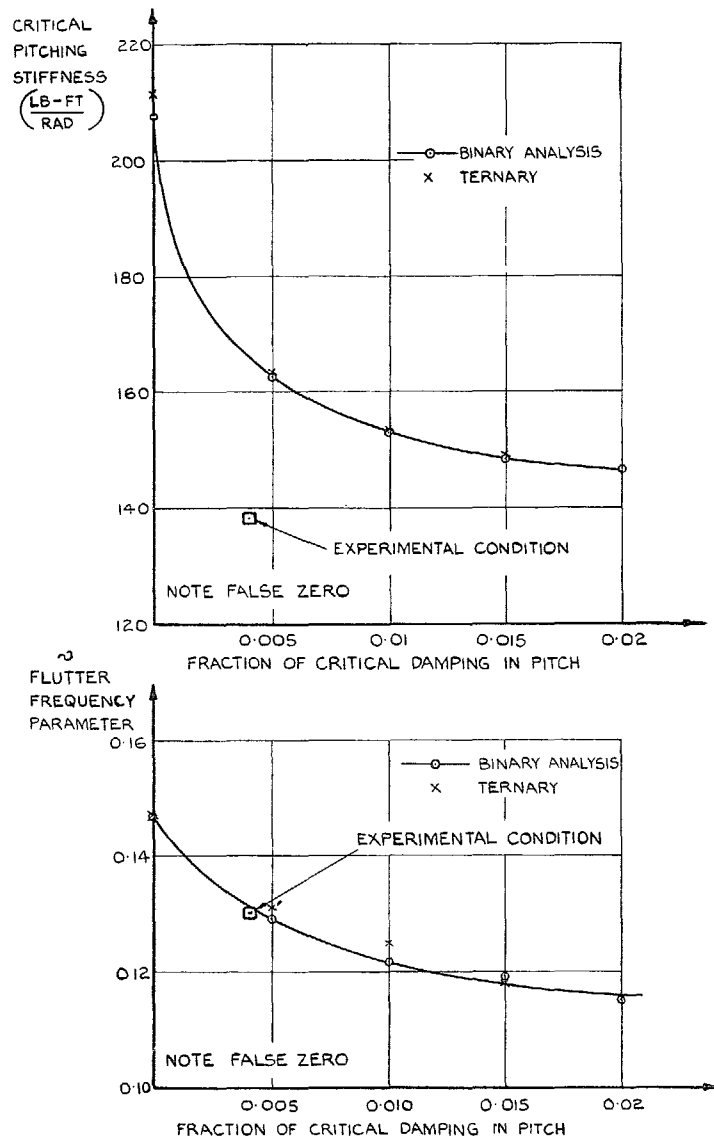


FIG. 7. Variation of flutter pitching stiffness and frequency parameter with structural damping in pitch for magnesium-alloy wing at $M = 1.6$ with pitching axis at the quarter-chord.

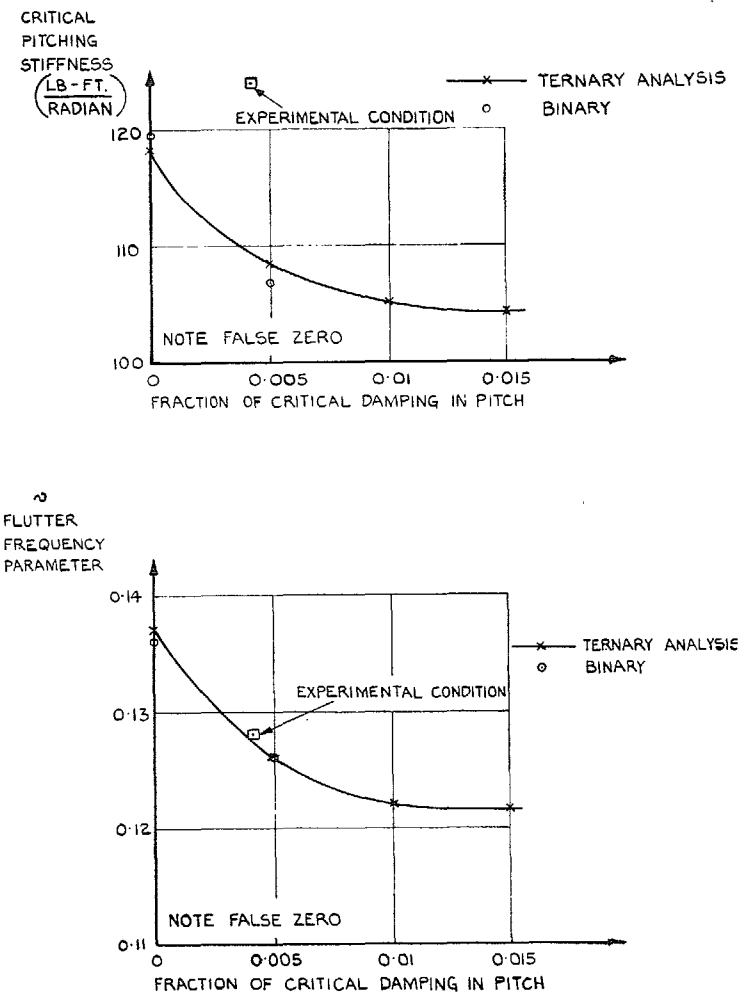
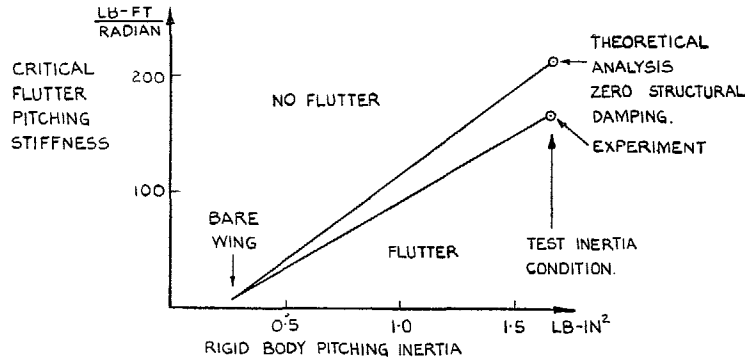
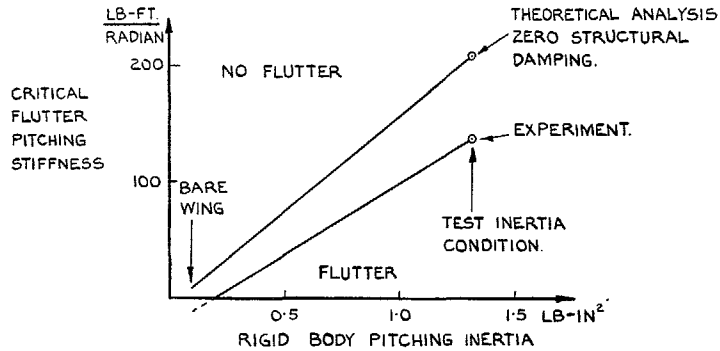


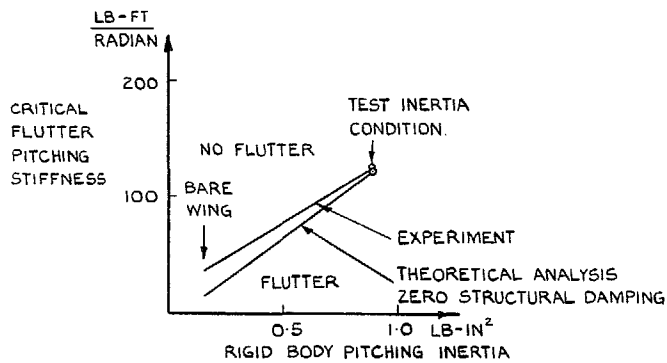
FIG. 8. Variation of flutter pitching stiffness and frequency parameter with structural damping in pitch for Duralumin wing at $M = 1.6$ with pitching axis at the quarter-chord.



(a) MAGNESIUM ALLOY WING : PITCHING AXIS AT LEADING EDGE.

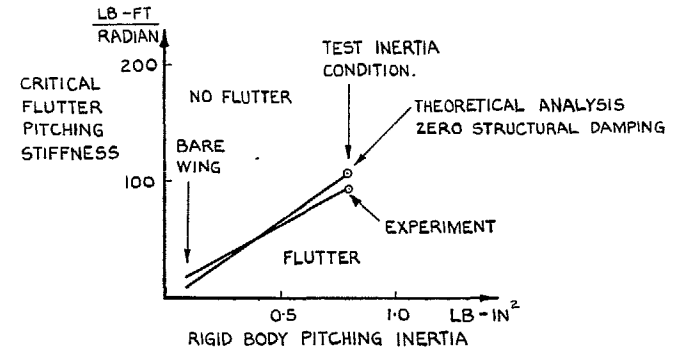


(b) MAGNESIUM ALLOY WING : PITCHING AXIS AT QUARTER CHORD.

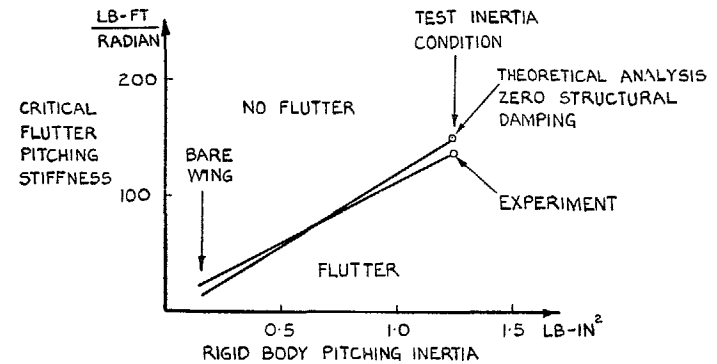


(c) DURALUMIN WING : PITCHING AXIS AT QUARTER CHORD.

Figs. 9a to 9c. Critical pitching stiffness vs. pitching inertia tests at $M = 1.6$.



(a) MAGNESIUM ALLOY WING : PITCHING AXIS AT QUARTER CHORD.



(b) DURALUMIN WING : PITCHING AXIS AT QUARTER CHORD.

Figs. 10a and 10b. Critical pitching stiffness vs. pitching inertia tests at $M = 2.0$.

Publications of the Aeronautical Research Council

ANNUAL TECHNICAL REPORTS OF THE AERONAUTICAL RESEARCH COUNCIL (BOUND VOLUMES)

- 1939 Vol. I. Aerodynamics General, Performance, Airscrews, Engines. 50s. (52s.).
Vol. II. Stability and Control, Flutter and Vibration, Instruments, Structures, Seaplanes, etc.
63s. (65s.)
- 1940 Aero and Hydrodynamics, Aerofoils, Airscrews, Engines, Flutter, Icing, Stability and Control,
Structures, and a miscellaneous section. 50s. (52s.)
- 1941 Aero and Hydrodynamics, Aerofoils, Airscrews, Engines, Flutter, Stability and Control,
Structures. 63s. (65s.)
- 1942 Vol. I. Aero and Hydrodynamics, Aerofoils, Airscrews, Engines. 75s. (77s.)
Vol. II. Noise, Parachutes, Stability and Control, Structures, Vibration, Wind Tunnels
47s. 6d. (49s. 6d.)
- 1943 Vol. I. Aerodynamics, Aerofoils, Airscrews. 80s. (82s.)
Vol. II. Engines, Flutter, Materials, Parachutes, Performance, Stability and Control, Structures.
90s. (92s. 9d.)
- 1944 Vol. I. Aero and Hydrodynamics, Aerofoils, Aircraft, Airscrews, Controls. 84s. (86s. 6d.)
Vol. II. Flutter and Vibration, Materials, Miscellaneous, Navigation, Parachutes, Performance,
Plates and Panels, Stability, Structures, Test Equipment, Wind Tunnels.
84s. (86s. 6d.)
- 1945 Vol. I. Aero and Hydrodynamics, Aerofoils. 130s. (132s. 9d.)
Vol. II. Aircraft, Airscrews, Controls. 130s. (132s. 9d.)
Vol. III. Flutter and Vibration, Instruments, Miscellaneous, Parachutes, Plates and Panels,
Propulsion. 130s. (132s. 6d.)
Vol. IV. Stability, Structures, Wind Tunnels, Wind Tunnel Technique. 130s. (132s. 6d.)

Annual Reports of the Aeronautical Research Council—

1937 2s. (2s. 2d.) 1938 1s. 6d. (1s. 8d.) 1939-48 3s. (3s. 5d.)

Index to all Reports and Memoranda published in the Annual Technical Reports, and separately—

April, 1950 - - - - R. & M. 2600 2s. 6d. (2s. 10d.)

Author Index to all Reports and Memoranda of the Aeronautical Research Council—

1909—January, 1954 R. & M. No. 2570 15s. (15s. 8d.)

Indexes to the Technical Reports of the Aeronautical Research Council—

December 1, 1936—June 30, 1939	R. & M. No. 1850	1s. 3d. (1s. 5d.)
July 1, 1939—June 30, 1945	R. & M. No. 1950	1s. (1s. 2d.)
July 1, 1945—June 30, 1946	R. & M. No. 2050	1s. (1s. 2d.)
July 1, 1946—December 31, 1946	R. & M. No. 2150	1s. 3d. (1s. 5d.)
January 1, 1947—June 30, 1947	R. & M. No. 2250	1s. 3d. (1s. 5d.)

Published Reports and Memoranda of the Aeronautical Research Council—

Between Nos. 2251-2349	R. & M. No. 2350	1s. 9d. (1s. 11d.)
Between Nos. 2351-2449	R. & M. No. 2450	2s. (2s. 2d.)
Between Nos. 2451-2549	R. & M. No. 2550	2s. 6d. (2s. 10d.)
Between Nos. 2551-2649	R. & M. No. 2650	2s. 6d. (2s. 10d.)
Between Nos. 2651-2749	R. & M. No. 2750	2s. 6d. (2s. 10d.)

Prices in brackets include postage

HER MAJESTY'S STATIONERY OFFICE

York House, Kingsway, London W.C.2; 423 Oxford Street, London W.1; 13a Castle Street, Edinburgh 2;
39 King Street, Manchester 2; 2 Edmund Street, Birmingham 3; 109 St Mary Street, Cardiff; Tower Lane, Bristol 1;
80 Chichester Street, Belfast, or through any bookseller.